One-pot synthesis of ANI@ZIF-8 for efficient photocatalytic degradation of RhB

Wenxing Niu, Ling Xue, Zhongnan Gao, Yunli Cao*, Yanqiu Wang, Qiuling Guo, Siyu Lou

School of Chemical and Environmental Engineering, Pingdingshan University, Pingdingshan 467000, China

Corresponding author*

E-mail address: yunlicao2008@163.com (Yunli Cao)

Abstract

Metal-organic frameworks (MOFs) are new porous crystalline materials that have shown excellent application potential in pollutant degradation. This study used a one-pot method to prepared the composite catalyst ANI@ZIF-8. XRD and SEM techniques were used to characterize the crystal structure and micromorphology. The performance of ANI@ZIF-8 and ZIF-8 as photocatalysts for the degradation of Rhodamine B (RhB) under UV light irradiation was also investigated. The results show that compared with pure ZIF-8, the ANI@ZIF-8 catalyst has a more outstanding photocatalytic degradation effect on RhB dye, with a degradation rate as high as 91.1%. This advantage stems from the electronic structural interaction between aniline and ZIF-8, which both promotes the excitation process of electrons and inhibits the recombination of photogenerated electrons and holes, thereby improving the photocatalytic efficiency. Free radical capture experiments confirmed that superoxide radicals and hydroxyl radicals are the main active species in the RhB degradation process. The results of the cyclic experiment indicate that, the ANI@ZIF-8 catalyst can be effectively reused five times, significantly

improving the economy of the process. Therefore, the ANI@ZIF-8 material provides a promising technological approach for the development of photocatalysts that can efficiently and stably treat wastewater organic pollutants.

Keywords: ZIF-8; encapsulating; aniline; photocatalytic; RhB

Introduction

With the rapid development of modern industry and the continuous acceleration of global industrialization, the problem of water pollution is deteriorating at an alarming rate and has become a critical environmental challenge restricting the sustainable development of human society, among which the discharge of organic dye wastewater is particularly prominent(Liang *et al.* 2018; Lin *et al.* 2024; Ren *et al.* 2024; Zheng *et al.* 2025; Abdipour and Asgari 2024). The textile and printing and dyeing industry, as the main source of organic dye wastewater, uses a large amount of various dyes in its production process(Khaliq *et al.* 2025; Ren et al. 2024; Viswanathan 2018; BLANCO-BRIEVA *et al.* 2024; Kamani *et al.* 2024). According to incomplete statistics, about 100000-150000 tons of dyes are discharged into the environment with wastewater every year worldwide(Jaihindh *et al.* 2025). These dyes not only color water bodies and damage natural landscapes, but also pose a serious threat to the ecological environment and human health(Liu *et al.* 2025; Lu *et al.* 2026). As a common organic dye, Rhodamine B is widely used in textile, printing and dyeing, food and other industries(Geng *et al.* 2025; Qi *et al.* 2025; Qin *et al.* 2025; Wang *et al.* 2025). It is highly toxic, difficult to degrade, and easy to accumulate in the environment. If it is directly discharged without effective treatment, it will cause irreversible damage to the

water ecosystem. The main methods for treating organic dye wastewater include flocculation(Chiavola *et al.* 2023; Maroli *et al.* 2024), adsorption(Song *et al.* 2022; Xiang *et al.* 2025), electrocatalysis(Dakave *et al.* 2024; Gajić *et al.* 2025) and photocatalysis(Huang, Zhu*, et al.* 2025; Saif *et al.* 2025). Among them, the flocculation method and the adsorption method can easily induce the risk of secondary pollution, and the electrocatalysis method faces the practical problem of high operating costs(Ahmad *et al.* 2018; Al-Tohamy *et al.* 2022). All three types of technologies have certain application limitations. In comparison, photocatalytic technology can use solar energy to completely degrade organic pollutants into harmless carbon dioxide and water. It has outstanding advantages such as high efficiency, environmental protection, and energy saving. It has become one of the current research hotspots in the field of organic dye wastewater treatment.(Chen *et al.* 2026; El Mouhri *et al.* 2026; Touili *et al.* 2026).

Many semiconductor photocatalysts, such as TiO_2(Anucha *et al.* 2022; Bertagna Silva and Marques 2025; Kaur *et al.* 2025), g-C_3N_4(Cai *et al.* 2025; Huang, Xu*, et al.* 2025; Khan *et al.* 2025; Mirzaei *et al.* 2025), ZnO(Hariharan 2006; Majumder *et al.* 2020; Morales-Flores *et al.* 2011; Silva *et al.* 2016), CdS(Haewon Byeon *et al.* 2025; Cheng *et al.* 2018; Nagamine *et al.* 2020; Repo *et al.* 2013) and $BiVO_4$(Nguyen *et al.* 2020; Pingmuang *et al.* 2017; Song *et al.* 2017), have been used to treat organic pollutants in wastewater. Among them, TiO_2, as the first-generation semiconductor photocatalyst, has attracted the interest of many researchers because of its stable chemical properties, good photocatalytic efficiency, non-toxicity, low cost and easy preparation. However, the application of TiO_2 photocatalysts in wastewater treatment

is limited due to low porosity, small specific surface area, and poor activity(Qu *et al.* 2013; Schneider *et al.* 2014). Poor adsorption capacity, difficult to recycle, narrow light response range, high selectivity for pollutants, and only utilizing ultraviolet light from sunlight. Therefore, there is a need to develop a semiconductor material with a slower carrier recombination speed and better light absorption ability in the UV visible region to replace TiO_2 photocatalyst.

MOFs materials, as an emerging class of porous materials, have enormous potential for applications in various fields, especially in the field of photocatalysis, where they have attracted much attention(Bétard and Fischer 2011; Fattah-alhosseini *et al.* 2024; Khan *et al.* 2023). Compared with other MOFs materials, ZIFs have the excellent properties of both zeolites and metal-organic frameworks, attracting the attention of a large number of researchers. Among many ZIFs, ZIF-8 is the most representative one, which not only has good specific surface area, thermal stability, chemical stability and water resistance, but also has adjustable porosity and abundant active sites(Lee *et al.* 2015; Tuncel and Ökte 2021; Wang *et al.* 2020). As is well known, ZIF-8 has excellent performance in adsorption, separation, catalysis, drug delivery and biosensors. Consequently, ZIF-8 derived composite materials are widely used and studied as catalysts in photocatalytic reactions.

In recent years, research has found that encapsulating functional molecules in the pores of MOFs can effectively modulate the electronic structure and photophysical properties of MOFs materials(Cui *et al.* 2016; Mancuso *et al.* 2020; Thaggard *et al.* 2022; Guo *et al.* 2023; Li *et al.* 2025). As an organic molecule with good photoelectric

properties, aniline contains conjugated π bonds in its molecular structure, which can absorb visible light and produce electronic transitions(Bhadra *et al.* 2009). At present, the photocatalytic degradation applications of ZIF-8 are mostly achieved by constructing heterojunctions with semiconductor materials (Elaouni *et al.* 2022). However, relevant research on coating aniline on ZIF-8 and using it as a photocatalyst has not yet been reported. Encapsulating aniline in ZIF-8 is expected to change the electron cloud distribution of ZIF-8, promote the separation of photogenerated electron-hole pairs, broaden its photoresponse range, and thus improve the photocatalytic ability of ZIF-8 to degrade organic pollutants. Based on this premise, this study successfully synthesized aniline-encapsulated ZIF-8 compounds using a one-pot method, systematically explored its photocatalytic degradation performance of Rhodamine B, revealed its photocatalytic reaction mechanism, provided solid theoretical support and practical guidance for the development of efficient and stable photocatalytic materials for organic dye wastewater treatment, and promoted the large-scale practical application of photocatalytic technology in the field of water pollution control.

2. Materials and Methods

2.1. Chemicals and Reagents

Zinc nitrate hexahydrate ($Zn(NO_3)_2 \cdot 6H_2O$, 99%), aniline ($C_6H_5N_2$, 99.5%), 2-methylimidazole ($C_4H_6N_2$, 99.8%), p-Benzoquinone ($C_6H_4O_2$, 98%), isopropyl alcohol (C_3H_8O, 99.7%) and triethanolamine ($C_6H_{15}NO_3$, 98%) were purchased from Sigma-Aldrich Co., Ltd. Methanol (CH_3OH, 99.5) and ethanol (C_2H_5OH, 95%) were obtained from Macklin Chemical Reagent Co., Ltd.. All the reagents were procured from

commercial suppliers and utilized directly without undergoing any additional purification or treatment procedures.

2.2. One-pot synthesis of ANI@ZIF-8

The preparation of ANI@ZIF-8 adhered to the subsequent experimental protocol (see Figure 1). In a standard ANI@ZIF-8 synthesis, 1.00 g of anilin and 0.60 g (2 mmol) of $Zn(NO_3)_2 \cdot 6H_2O$ were dissolved in 20 mL of methanol. Meanwhile, 0.65 g (8 mmol) of 2-methylimidazole was dissolved in a separate 20 mL of methanol. Subsequently, these two solutions were combined. The resulting mixture was continuously stirred at ambient temperature for 24 hours. The generated white precipitate was harvested via centrifugation and repeatedly rinsed with ethanol to thoroughly eliminate the residual 2-methylimidazole. Ultimately, the sample was dried at room temperature. For comparison, ZIF-8 was prepared by the same synthesis procedure as above, but in the absence of ANI.

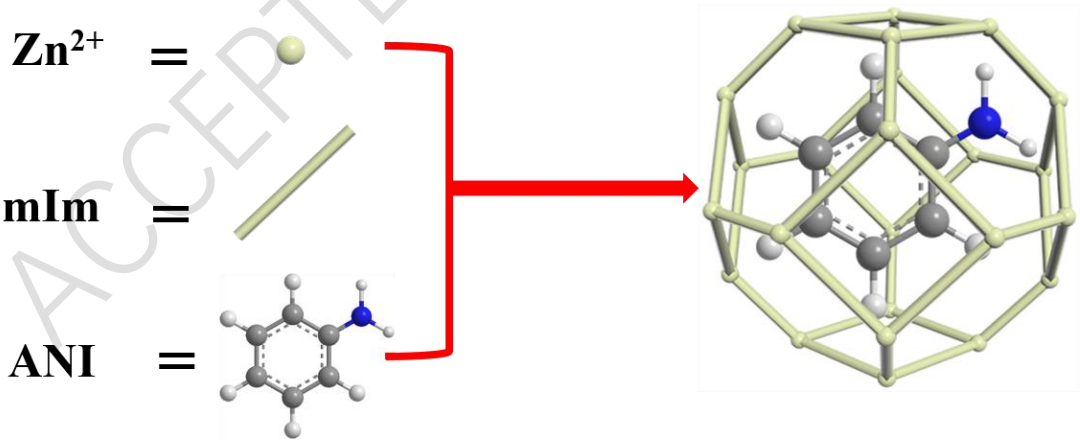

Figure 1 Schematic illustration of the one-pot preparation of ANI@ZIF-8

2.3. Characterization

The powder X-ray diffraction (PXRD) patterns of the samples were measured by

an X-ray diffractometer (Rigaku, MiniFlex II) equipped with monochromated Cu-Kα radiation (λ = 1.5418 Å). The crystal morphology and size were examined Via scanning electron microscopy (SEM; Hitachi, SU8010).

2.4 Photocatalytic Degradation Experiment

The photocatalytic degradation performance of ZIF-8 and ANI@ZIF-8 was investigated under visible light. The rhodamine B solution was used as a simulated polluted water sample. In a dark environment, the suspension was stirred at a speed of 600 revolutions per minute for 30 minutes to reach the adsorption/desorption equilibrium state. For photocatalysis, the RhB solution containing the photocatalyst was exposed to a 500-watt xenon lamp, with a fixed distance maintained between the light source and the light reaction chamber. At 0–30 minute intervals, 5 mL aliquots of the solution were collected via syringe, centrifuged to separate the supernatant from the photocatalyst, and analyzed using a UV-Visible spectrometer at 554 nm (Figure 2a). The residual RhB concentration was determined using a calibration curve ($Y = 0.0291X - 0.0009$, $R^2 = 0.9999$) (Figure 2b). The photocatalytic degradation efficiency (%) was calculated using Equation (1), where C_0 (mg L^{-1}) and C_t (mg L^{-1}) denote the initial and time-dependent dye concentrations, respectively:

$$\text{Photocatalytic degradation (\%)} = (C_0 - C_t)/C_0 \times 100$$

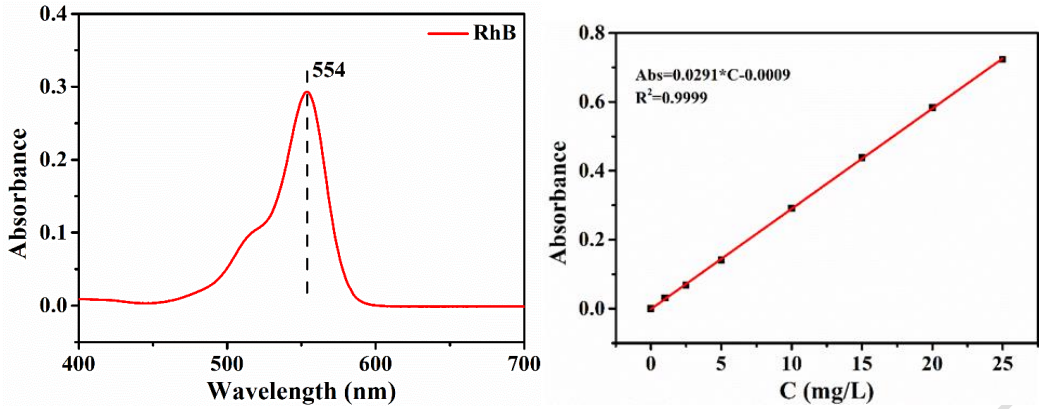

Figure 2 (a) UV-vis absorbances for RhB under visable light irradiation, (b) standard curve of RhB

2.5 Role of Radical Trapping Scavengers

In a photocatalysis experiment, various radical scavengers were employed to explore their respective contributions during the photocatalytic degradation process. Prior to reaching the adsorption-desorption equilibrium phase, active trapping agents (p-Benzoquinone, isopropyl alcohol, triethanolamine), namely BQ, TPA and TEOA, were added to the solution under identical experimental settings. These reagents are specifically designed to capture superoxide free radicals, hydroxyl free radicals and holes.

2.6 Recycling of Photocatalyst

In order to systematically evaluate the stability and cyclability of samples in the photocatalytic degradation system, this study designed and carried out five rounds of cyclic experiments. After each round of RhB dye photocatalytic degradation reaction, the photocatalyst was recovered and washed three times with ultrapure water to completely remove surface adsorbed impurities, and then dried in a constant temperature oven at 60°C for 12 hours. After drying, it was sealed and stored in a sealed

bottle for subsequent cycle experiments.

3. Results and Discussion

3.1. Powder X-ray diffraction (PXRD)

Figure 3 shows the XRD patterns of ZIF-8 and ANI@ZIF-8. It can be seen that the peak position of the characteristic peak of ANI@ZIF-8 is highly consistent with that of the parent ZIF-8, indicating that the crystal structure of ZIF-8 was not damaged during the in-situ encapsulation process of ANI molecules. This indicates that the crystal structure of ZIF-8 was not damaged during the in-situ encapsulation process of ANI molecules. Furthermore, the comparison found that the diffraction peak intensity of ANI@ZIF-8 at 2θ=7.36° is significantly weaker than that of the parent ZIF-8. This result further confirms that ANI has been successfully encapsulated within the ZIF-8 crystal structure.

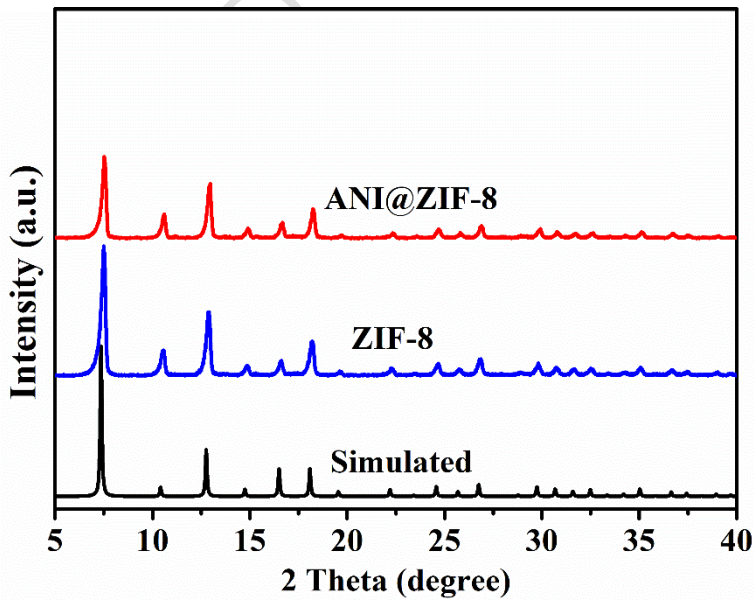

Figure 3. PXRD patterns of ZIF-8 and ANI@ZIF-8

3.2 Scanning electron microscopy (SEM)

Figure 4 shows the SEM images of ZIF-8 and ANI@ZIF-8. As shown in the Figure 4, both materials exhibit unique polyhedral geometry, and the particle size of ANI@ZIF-8 is significantly larger than that of pure ZIF-8. This indicates that the encapsulation process of aniline molecules within the ZIF-8 framework does not affect its original morphology and only increases the particle size.

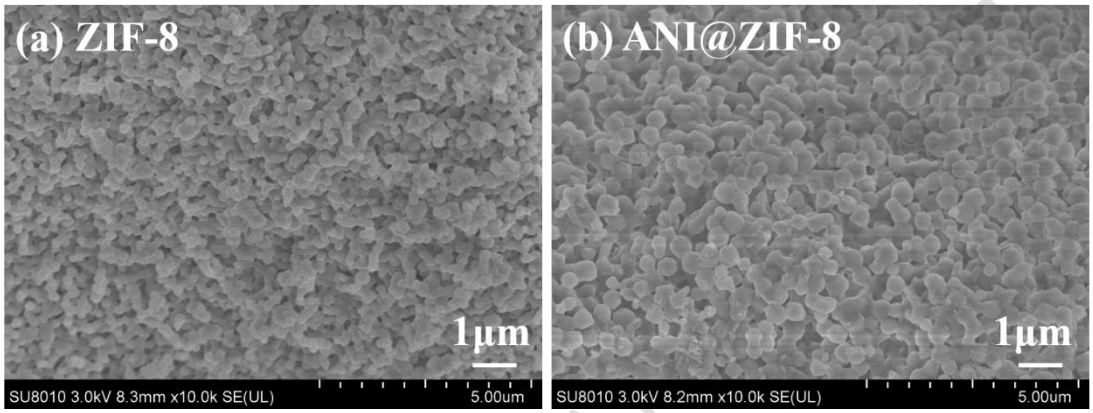

Figure 4. SEM images and EDS spectra of ZIF-8 (a) and ANI@ZIF-8

3.3 Photocatalytic Degradation Performance

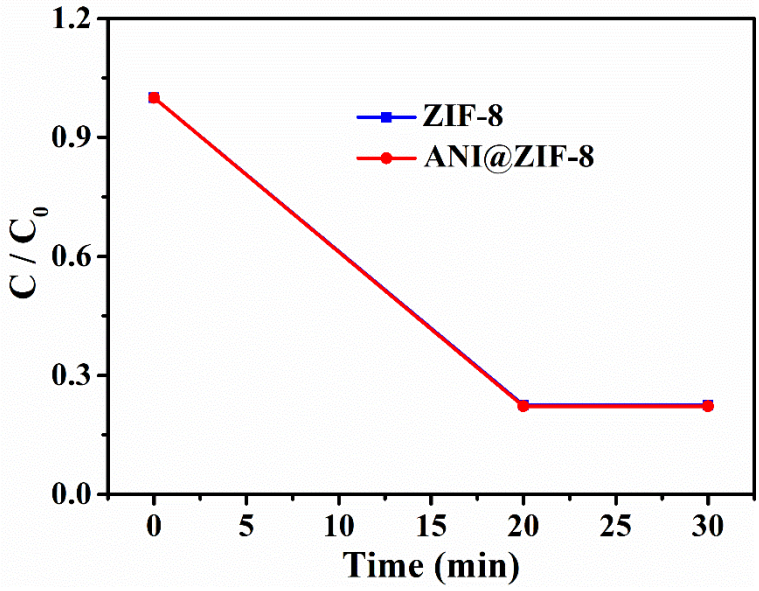

Figure 5 The adsorption performance of RhB by ZIF-8 and ANI@ZIF-8 under dark conditions

Under normal temperature and in the absence of light, the adsorption performance of ZIF-8 and ANI@ZIF-8 for rhodamine B is shown in Figure 5. It can be seen that the addition of both materials can significantly improve the adsorption effect of RhB, and the adsorption amount increases with the extension of adsorption time. When the adsorption time reaches 30 minutes, the adsorption amount tends to be stable and reaches the maximum value. Therefore, it was finally determined that the adsorption pretreatment conditions before subsequent photocatalytic reactions were: adsorption at room temperature in the dark for 30 minutes.

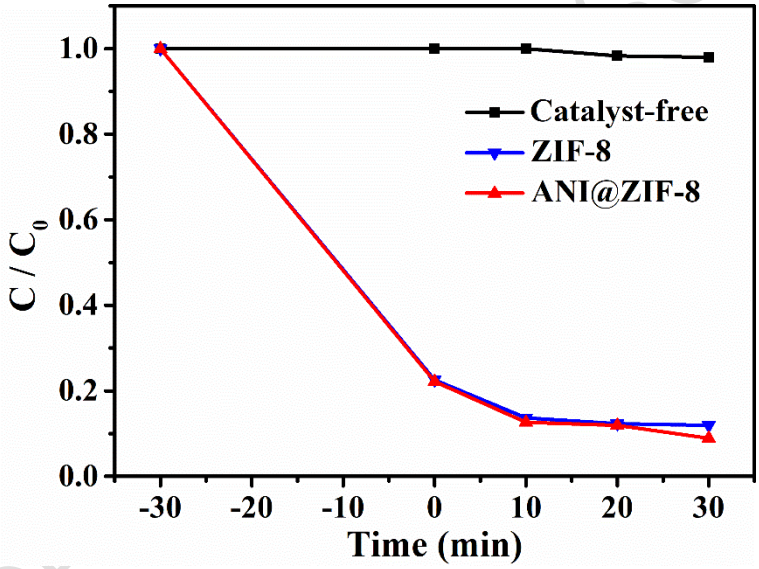

Figure 6 The degradation of RhB under the conditions of ZIF-8 and ANI@ZIF-8 catalysts

Figure 6 shows the experimental curve of photocatalytic degradation of RhB dye by 50 mg ZIF-8 and ANI@ZIF-8. As shown in the Figure 6, both samples can effectively degrade RhB. However, the degradation effect of ANI@ZIF-8 was significantly better than that of pure ZIF-8. After 30 minutes of reaction, the degradation rate of ANI@ZIF-8 is as high as 91.1%, which basically achieving complete

degradation of RhB. This indicates that the aniline encapsulation modification has a significant improvement effect on the catalytic performance of ZIF-8.

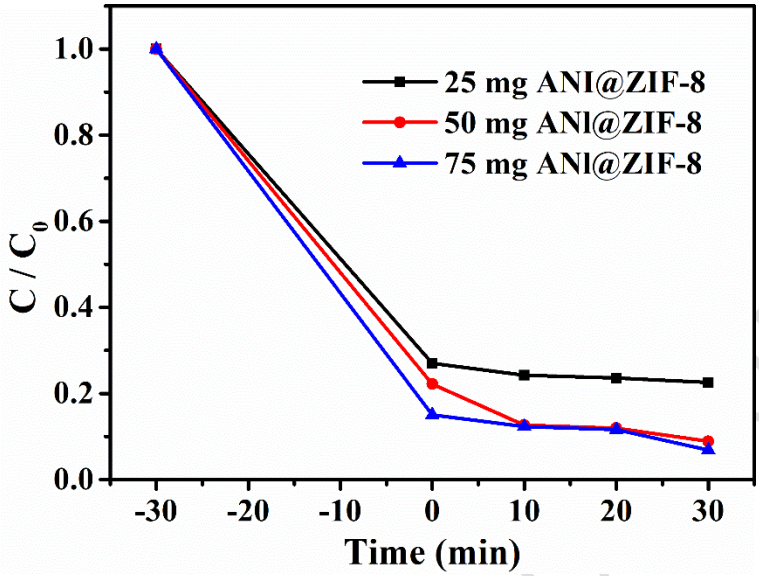

Figure 7 The RhB degradation graphs under different addition amounts of ANI@ZIF-8

Figure 7 shows different concentrations of ANI@ZIF-8 Comparison of catalytic degradation effects of RhB pollutant solution. It can be seen that within a certain concentration range, the catalytic effect of the new composite material ANI@ZIF-8 on RhB increases as the catalyst concentration increases. The higher the concentration, the better the catalytic effect. Among them, the removal rates of RhB by 25 mg, 50 mg, and 75 mg ANI@ZIF-8 were 77.5%, 91.1%, and 93.2% respectively, which shows that increasing the catalyst concentration can significantly improve the degradation efficiency, while there is no significant difference in the degradation effect between 50 mg and 75 mg concentrations.

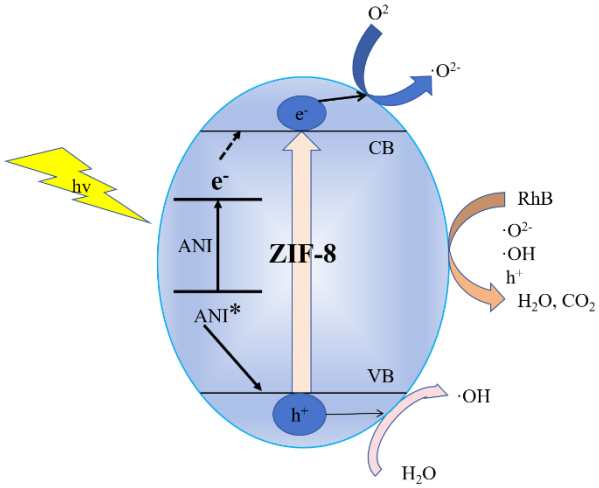

Figure 8 Photocatalytic Degradation Mechanism Diagram photocatalytic mechanism

The photocatalytic reaction mechanism is as follows (see Figure 8): under light conditions, the aniline molecules encapsulated in ZIF-8 are first excited by light to form excited state aniline (*aniline). The electrons of excited aniline can be transferred to the conduction band (CB) of ZIF-8 to achieve spatial separation of electrons, while the corresponding holes remain on the excited aniline. In addition, the conjugated structure of aniline molecules can interact with the electronic structure of ZIF-8, regulating the electron excitation process and effectively suppressing the recombination of photo generated electron hole pairs, thereby enhancing the photocatalytic degradation efficiency of RhB solution.

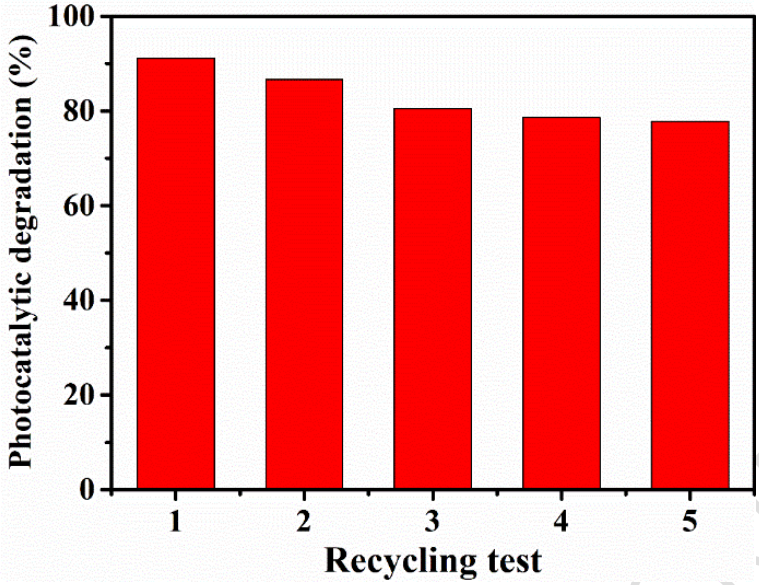

Figure 9 Reusability of radicals of ANI@ZIF-8 composite in photocatalytic degradation process

The photocatalytic reusability performance of the prepared sample was evaluated through five cycle experiments, and the results are shown in Figure 9. The photocatalytic performance of the ANI@ZIF-8 material decreased slightly during the cycle test, which is speculated to be related to the detachment of nanoparticles during the washing process. Nevertheless, its photocatalytic degradation rate of RhB can still reach 77.8%.

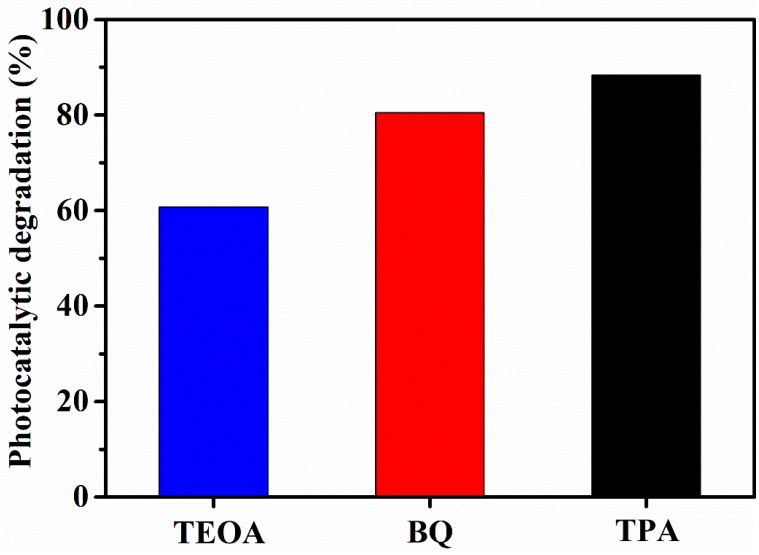

Figure 10 Role of radicals of ANI@ZIF-8 composite in photocatalytic degradation process

In order to explore the mechanism of active components of ANI@ZIF-8 composites, this study used free radical capture experiments to analyze the key active components in the photocatalytic degradation of RhB. In the experiment, benzoquinone (BQ), triethanolamine (TEOA), and isopropanol (IPA) were used as quenchers for superoxide radicals (O_2^-), holes (h^+), and hydroxyl radicals (· OH), respectively. The results are shown in Figure 10. It can be seen that after the addition of BQ and IPA, the RhB degradation efficiency decreased from 91.1% to 80.5% and 60.7%, respectively, while the degradation rate of the TEOA system only slightly decreased to 88.3%. This shows that O_2^- and ·OH play a dominant role in the photocatalytic reaction, with a relatively small contribution from h^+. The organic pollutants are eventually oxidized and decomposed into CO_2, H_2O and small molecular compounds.

Conclusion

In this study, ANI@ZIF-8 composite was synthesized using a one-pot method, its phase and morphology were systematically characterized by XRD and SEM, and it was used as a photocatalytic material in the degradation experiment of RhB. The results show that (1) the conjugated structure of aniline molecules can interact with the electronic structure of ZIF-8, regulating the electron excitation process and effectively suppressing the recombination of photo generated electron hole pairs. (2) ANI@ZIF-8, as a photocatalyst, has a degradation rate of 91.1% for RhB, which is significantly better than pure ZIF-8. (3) In the photocatalytic degradation reaction, O_2^- and ·OH free radicals play a dominant role. (4) After five cycles of use, the degradation rate of RhB by the compound still reached 77.8%, indicating that the compound has excellent stability, effectiveness and economy. In summary, the successful synthesis of ANI@ZIF-8 provides a useful reference for the development of efficient, practical

and economical photocatalysts, and has good application prospects in the treatment of organic dyes in textile wastewater in the future.

This study was supported by the Pingdingshan University's Ph.D. Research Startup Fund Project (grant number PXY-BSQD-2023009)and the Science and Technology Public Relations Project of Henan Province (grant number 252102230087).

Reference

Abdipour, H., and Asgari, G. (2024). Enhanced methylene blue degradation and miniralization through activated persulfate coupled with magnetic field. *Cleaner Engineering and Technology*, **23**, doi 10.1016/j.clet.2024.100822.

Ahmad, Y. H., Mohamed, A. T., Sliem, M. H., Abdullah, Aboubakr M., and Al-Qaradawi, S. Y. (2018). Enhanced photocatalytic performance of WON@porous TiO_2 nanofibers towards sunlight-assisted degradation of organic contaminants. *RSC Advances*, **8** (57):32747–55, doi 10.1039/c8ra06477f.

Al-Tohamy, R., Ali, S. S., Li, F., Okasha, K. M., Mahmoud, Y. A. G., Elsamahy, T., Jiao, H., Fu, Y., and Sun, J. (2022). A critical review on the treatment of dye-containing wastewater: Ecotoxicological and health concerns of textile dyes and possible remediation approaches for environmental safety. *Ecotoxicology and Environmental Safety*, **231**, doi 10.1016/j.ecoenv.2021.113160.

Anucha, C. B., Altin, I., Bacaksiz, E., and Stathopoulos, V. N. (2022). Titanium dioxide (TiO_2)-based photocatalyst materials activity enhancement for contaminants of emerging concern (CECs) degradation: In the light of modification strategies. *Chemical Engineering Journal Advances*, **10**, doi 10.1016/j.ceja.2022.100262.

Bertagna Silva, D., and Marques, A. C. (2025). TiO_2-based photocatalytic degradation of microplastics in water: Current status, challenges and future perspectives. *Journal of Water Process Engineering*, **72**, doi 10.1016/j.jwpe.2025.107465.

Bétard, A., and Fischer, R. A. (2011). Metal–Organic Framework Thin Films: From Fundamentals to Applications. *Chemical Reviews*, **112** (2):1055–83, doi 10.1021/cr200167v.

Bhadra, S., Khastgir, D., Singha, N. K., and Lee, J. H. (2009). Progress in preparation, processing and applications of polyaniline. *Progress in Polymer Science*, **34** (8):783–810, doi 10.1016/j.progpolymsci.2009.04.003.

BLANCO-BRIEVA, G., CAMPOS-MARTIN, J. M., AL-ZAHRANI, S. M., and FIERRO, J. L. G. (2024). REMOVAL OF REFRACTORY ORGANIC SULFUR COMPOUNDSIN FOSSIL FUELS USING MOF SORBENTS. *Global NEST Journal*, **12** (3):296–304.

Cai, C., Shi, J., Liu, Q., Zhu, Q., Fu, Q., Wang, W., and Duan, X. (2025). Efficient activation of peracetic acid by Fe-doped g-C_3N_4 for selective degradation of emerging contaminants: Unraveling the role of reactive complex. *Journal of Hazardous Materials*, **497**, doi 10.1016/j.jhazmat.2025.139666.

Chen, Z., Meng, F., Zhu, D., and Fu, M. (2026). Chitosan/g-C_3N_4/graphene oxide aerogel for efficient removal of rhodamine B and bisphenol A. *Materials Science and Engineering: B*, **323**, doi 10.1016/j.mseb.2025.118882.

Cheng, L., Xiang, Q., Liao, Y., and Zhang, H. (2018). CdS-Based photocatalysts. *Energy & Environmental Science*, **11** (6):1362–91, doi 10.1039/c7ee03640j.

Chiavola, A., Di Marcantonio, C., D'Agostini, M., Leoni, S., and Lazzazzara, M. (2023). A

combined experimental-modeling approach for turbidity removal optimization in a coagulation–flocculation unit of a drinking water treatment plant. *Journal of Process Control*, **130**, doi 10.1016/j.jprocont.2023.103068.

Cui, Y., Li, B., He, H., Zhou, W., Chen, B., and Qian, G. (2016). Metal–Organic Frameworks as Platforms for Functional Materials. *Accounts of Chemical Research*, **49** (3):483–93, doi 10.1021/acs.accounts.5b00530.

Dakave, S., Bhinge, G., and Kanamadi, C. (2024). Dual-capable spinel cobalt oxide nanoparticles for electrocatalytic oxygen evolution and water contaminant removal. *Environmental Science and Pollution Research*, **32** (37):22051–63, doi 10.1007/s11356-024-34682-z.

El Mouhri, W., Nadif, I., Tajat, N., El Hayaoui, W., Idlahcen, A., Talebi, J., Bakas, I., Qourzal, S., Assabbane, A., and Tamimi, M. (2026). Mechanochemical synthesis of AgI–BiOI@g-C_3N_4 heterojunction for the efficient degradation of cationic dye RhB under visible light irradiation. *Journal of Physics and Chemistry of Solids*, **208**, doi 10.1016/j.jpcs.2025.113013.

Elaouni, A., El Ouardi, M., Zbair, M., BaQais, A., Saadi, M., and Ait Ahsaine, H. (2022). ZIF-8 metal organic framework materials as a superb platform for the removal and photocatalytic degradation of organic pollutants: a review. *RSC Advances*, **12** (49):31801–17, doi 10.1039/d2ra05717d.

Fattah-alhosseini, A., Sangarimotlagh, Z., Karbasi, M., and Kaseem, M. (2024). Review of MXene/MOF composites as photocatalysts for pollutant degradation. *Nano-Structures & Nano-Objects*, **38**, doi 10.1016/j.nanoso.2024.101192.

Gajić, B., Milošević, M., Kepić, D., Ćirić-Marjanović, G., Šaponjić, Z., and Radoičić, M. (2025). Carbon-Rich Nanocomposites Based on Polyaniline/Titania Nanotubes Precursor: Synergistic Effect Between Surface Adsorption and Photocatalytic Activity. *Molecules*, **30** (12), doi 10.3390/molecules30122628.

Geng, S., Sui, X., Li, Y., Wang, H., Zhao, X., Chang, L., and Duan, X. (2025). Reinforcing piezo-photocatalytic properties and enhancing RhB degradation efficiency of Ce-doped $Bi_4Ti_3O_{12}$: mechanistic insights. *Journal of Materials Chemistry A*, **13** (29):23838–52, doi 10.1039/d5ta02788h.

Guo, L., Chen, W., Wang, C., and Dong, B. (2023). Application of electrochemically assisted synthesis of MOFs-derived phosphides as catalyst for CH_4-CO_2 reforming. *International Journal of Electrochemical Science*, **18** (1):26–32, doi 10.1016/j.ijoes.2023.01.005.

Haewon Byeon, Priyanshu Kumar Singh, N. Shalom, M. Sivaprakash, Prakash A, Sudherson, D. P. S., and J, n. S. (2025). A Study on the potential industrial effluent remediation applications of CdS nanoparticles through niobium incorporation. *Global NEST Journal*, **27** (4):07140, doi 10.30955/gnj.07140.

Hariharan, C. (2006). Photocatalytic degradation of organic contaminants in water by ZnO nanoparticles: Revisited. *Applied Catalysis A: General*, **304**:55–61, doi 10.1016/j.apcata.2006.02.020.

Huang, B., Xu, K., Zhao, Y., Li, B., Jiang, S., Liu, Y., Huang, S., Yang, Q., Gao, T., Xie, S., Chen, H., and Li, Y. (2025). Review of the Versatility and Application Potentials of g-C_3N_4-Based S-Scheme Heterojunctions in Photocatalytic Antibiotic Degradation.

Molecules, **30** (6), doi 10.3390/molecules30061240.

Huang, Z., Zhu, P., Liu, M., Xin, X., He, B., and Li, X. (2025). Photocatalytic degradation of norfloxacin antibiotic by a novel Cu-ZnO/BiOI/Bi_2WO_6 double Z-type heterojunction: Performance, mechanism insight and toxicity assessment. *Separation and Purification Technology*, **356**, doi 10.1016/j.seppur.2024.129959.

Jaihindh, D. P., Lin, Y.-F., Tseng, L.-H., Krisbiantoro, P. A., Wu, K. C. W., Shukla, K., Sone, M., Chang, T.-F. M., and Chen, C.-Y. (2025). Heterogeneous Z-scheme CuO/ZnO aerogel photocatalyst for photocatalytic degradation of organic dye. *Journal of the Taiwan Institute of Chemical Engineers*, **175**, doi 10.1016/j.jtice.2025.106281.

Kamani, H., Hosseinzehi, M., Ghayebzadeh, M., Azari, A., Ashrafi, S. D., and Abdipour, H. (2024). Degradation of reactive red 198 dye from aqueous solutions by combined technology advanced sonofenton with zero valent iron: Characteristics/ effect of parameters/kinetic studies. *Heliyon*, **10** (1), doi 10.1016/j.heliyon.2023.e23667.

Kaur, B., Singh, P., Thakur, S., Singh, A., Chaudhary, V., Kumar, N., Khan, A. A. P., Rub, M. A., Azum, N., and Raizada, P. (2025). Harnessing 3D printing for tailored TiO_2 structures redefining organic pollutant degradation. *Journal of Environmental Chemical Engineering*, **13** (2), doi 10.1016/j.jece.2025.116042.

Khaliq, H., Adnan, M., Usman, M., Shahzad, F., Nadeem, A., Shazly, G. A., Ashraf, G. A., and Zhao, Z. (2025). Fabrication of Novel ZnO@Mn_3C photocatalyst for organic pollutants degradation via peroxymonosulfate activation. *Materials Science in Semiconductor Processing*, **192**, doi 10.1016/j.mssp.2025.109425.

Khan, M. D., Farooq, M. u. H., Fareed, I., Khan, M. F., Rehman, Z. U., Ayoub, U., Ahmed, A.,

and Butt, F. K. (2025). Novel N-doped ZnO and O-doped g-C_3N_4 heterojunction: Enhanced photocatalytic degradation and robust electrochemical biosensing of ascorbic acid. *Diamond and Related Materials*, **151**, doi 10.1016/j.diamond.2024.111752.

Khan, M. S., Li, Y., Li, D.-S., Qiu, J., Xu, X., and Yang, H. Y. (2023). A review of metal–organic framework (MOF) materials as an effective photocatalyst for degradation of organic pollutants. *Nanoscale Advances*, **5** (23):6318–48, doi 10.1039/d3na00627a.

Lee, Y.-R., Jang, M.-S., Cho, H.-Y., Kwon, H.-J., Kim, S., and Ahn, W.-S. (2015). ZIF-8: A comparison of synthesis methods. *Chemical Engineering Journal*, **271**:276–80, doi 10.1016/j.cej.2015.02.094.

Li, Y., Bu, J., Sun, Y., Huang, Z., Zhu, X., Li, S., Chen, P., Tang, Y., He, G., and Zhong, S. (2025). Efficient degradation of norfloxacin by synergistic activation of PMS with a three-dimensional electrocatalytic system based on Cu-MOF. *Separation and Purification Technology*, **356**, doi 10.1016/j.seppur.2024.129945.

Liang, H., Liu, S., Zhang, H., Wang, X., and Wang, J. (2018). New insight into the selective photocatalytic oxidation of RhB through a strategy of modulating radical generation. *RSC Advances*, **8** (24):13625–34, doi 10.1039/c8ra01810c.

Lin, X., Chen, Y., Zhou, D., Chen, M., Liang, W., and Guo, H. (2024). Aminated graphene quantum dots/CdS nanobelts for enhanced photocatalytic degradation of RhB dye under visible light. *RSC Advances*, **14** (1):255–65, doi 10.1039/d3ra06454a.

Liu, Y., Hu, H., Chen, C., and Xu, L. (2025). Rapid Decoloration of Rhodamine B in Fe(III)/Peroxymonosulfate Process in Presence of Ascorbic Acid. *Water, Air, & Soil*

Pollution, **237** (1), doi 10.1007/s11270-025-08712-6.

Lu, J.-F., Wang, H., Zhou, Y., Mao, X.-Y., Feng, X.-Q., Wang, S., and Zhao, Y.-H. (2026). Degradation of rhodamine B by fenton-like system with Fe-Cu/HZSM-5 catalyst. *Journal of the Taiwan Institute of Chemical Engineers*, **178**, doi 10.1016/j.jtice.2025.106412.

Majumder, S., Chatterjee, S., Basnet, P., and Mukherjee, J. (2020). ZnO based nanomaterials for photocatalytic degradation of aqueous pharmaceutical waste solutions – A contemporary review. *Environmental Nanotechnology, Monitoring & Management*, **14**, doi 10.1016/j.enmm.2020.100386.

Mancuso, J. L., Mroz, A. M., Le, K. N., and Hendon, C. H. (2020). Electronic Structure Modeling of Metal–Organic Frameworks. *Chemical Reviews*, **120** (16):8641–715, doi 10.1021/acs.chemrev.0c00148.

Maroli, A. S., Zhang, Y., Lubiantoro, J., and Venkatesan, A. K. (2024). Surfactant-enhanced coagulation and flocculation improves the removal of perfluoroalkyl substances from surface water. *Environmental Science: Advances*, **3** (12):1714–21, doi 10.1039/d4va00093e.

Mirzaei, H., Ehsani, M. H., and Shakeri, A. (2025). Development and characterization of a graphene quantum dot/g-C_3N_4 photocatalyst for efficient degradation of Rhodamine B. *Scientific Reports*, **15** (1), doi 10.1038/s41598-025-13373-w.

Morales-Flores, N., Pal, U., and Sánchez Mora, E. (2011). Photocatalytic behavior of ZnO and Pt-incorporated ZnO nanoparticles in phenol degradation. *Applied Catalysis A: General*, **394** (1-2):269–75, doi 10.1016/j.apcata.2011.01.011.

Nagamine, M., Osial, M., Jackowska, K., Krysinski, P., and Widera-Kalinowska, J. (2020). Tetracycline Photocatalytic Degradation under CdS Treatment. *Journal of Marine Science and Engineering*, **8** (7), doi 10.3390/jmse8070483.

Nguyen, T. D., Nguyen, V.-H., Nanda, S., Vo, D.-V. N., Nguyen, V. H., Van Tran, T., Nong, L. X., Nguyen, T. T., Bach, L.-G., Abdullah, B., Hong, S.-S., and Van Nguyen, T. (2020). $BiVO_4$ photocatalysis design and applications to oxygen production and degradation of organic compounds: a review. *Environmental Chemistry Letters*, **18** (6):1779–801, doi 10.1007/s10311-020-01039-0.

Pingmuang, K., Chen, J., Kangwansupamonkon, W., Wallace, G. G., Phanichphant, S., and Nattestad, A. (2017). Composite Photocatalysts Containing $BiVO_4$ for Degradation of Cationic Dyes. *Scientific Reports*, **7** (1), doi 10.1038/s41598-017-09514-5.

Qi, N., Xin, X., Ji, D., Jia, R., and Li, Y. (2025). Construction of eco-friendly ZnO-chitosan photocatalyst toward enhanced RhB degradation performance. *Materials Science and Engineering: B*, **321**, doi 10.1016/j.mseb.2025.118461.

Qin, Y., Peng, X., Wu, T., Zhong, Y., Xu, H., Mao, Z., and Zhang, L. (2025). Construction of BiOBr/BNQDs Heterostructure Photocatalyst and Performance Studies of Photocatalytic Degradation of RhB. *Catalysts*, **15** (8), doi 10.3390/catal15080771.

Qu, X., Alvarez, P. J. J., and Li, Q. (2013). Applications of nanotechnology in water and wastewater treatment. *Water Research*, **47** (12):3931–46, doi 10.1016/j.watres.2012.09.058.

Ren, X., Chu, Y., Yuan, S., Zheng, Y., Zeng, Z., Xia, C., Zhao, L., Wu, Y., and He, Y. (2024). Enhanced piezocatalytic RhB degradation with $ZnSnO_3$ Nanocube-modified

$Bi_4Ti_3O_{12}$ composite catalyst by harnessing ultrasonic energy. *Journal of Environmental Management*, **370**:122776, doi 10.1016/j.jenvman.2024.122776.

Repo, E., Rengaraj, S., Pulkka, S., Castangnoli, E., Suihkonen, S., Sopanen, M., and Sillanpää, M. (2013). Photocatalytic degradation of dyes by CdS microspheres under near UV and blue LED radiation. *Separation and Purification Technology*, **120**:206–14, doi 10.1016/j.seppur.2013.10.008.

Saif, A., Rizvi, S. I., Shaukat, Z., Saif, M., Tabassum, S., Khalid, R., Javed, F., Rebouh, N. Y., Hassan, F., and Zaman, Q. u. (2025). Development of composite catalyst containing renewable biochar blended with zinc oxide and copper diphenyl amine for visible light photocatalytic degradation of methylene blue. *Frontiers in Sustainable Food Systems*, **9**, doi 10.3389/fsufs.2025.1500907.

Schneider, J., Matsuoka, M., Takeuchi, M., Zhang, J., Horiuchi, Y., Anpo, M., and Bahnemann, D. W. (2014). Understanding TiO_2 Photocatalysis: Mechanisms and Materials. *Chemical Reviews*, **114** (19):9919–86, doi 10.1021/cr5001892.

Silva, I. M. P., Byzynski, G., Ribeiro, C., and Longo, E. (2016). Different dye degradation mechanisms for ZnO and ZnO doped with N (ZnO:N). *Journal of Molecular Catalysis A: Chemical*, **417**:89–100, doi 10.1016/j.molcata.2016.02.027.

Song, X., Li, Y., Wei, Z., Ye, S., and Dionysiou, D. D. (2017). Synthesis of $BiVO_4$/P25 composites for the photocatalytic degradation of ethylene under visible light. *Chemical Engineering Journal*, **314**:443–52, doi 10.1016/j.cej.2016.11.164.

Song, Y., Wang, K., Zhao, F., Du, Z., Zhong, B., and An, G. (2022). Preparation of Powdered Activated Carbon Composite Material and Its Adsorption Performance and

Mechanisms for Removing RhB. *Water*, **14** (19), doi 10.3390/w14193048.

Thaggard, G. C., Haimerl, J., Park, K. C., Lim, J., Fischer, R. A., Maldeni Kankanamalage, B. K. P., Yarbrough, B. J., Wilson, G. R., and Shustova, N. B. (2022). Metal–Photoswitch Friendship: From Photochromic Complexes to Functional Materials. *Journal of the American Chemical Society*, **144** (51):23249–63, doi 10.1021/jacs.2c09879.

Touili, S., Asbani, B., Hadouch, Y., Amjoud, M. b., Mezzane, D., Suban, N., Uršič, H., Rajput, N. S., Kutnjak, Z., Rožič, B., Jouiad, M., and Marssi, M. E. (2026). Ferroelectric KNbO3 nanoplatelets for thermally driven pyrocatalytic hydrogen evolution and dye degradation. *Fuel*, **405**, doi 10.1016/j.fuel.2025.136705.

Tuncel, D., and Ökte, A. N. (2021). Improved Adsorption Capacity and Photoactivity of ZnO-ZIF-8 Nanocomposites. *Catalysis Today*, **361**:191–97, doi 10.1016/j.cattod.2020.04.014.

Viswanathan, B. (2018). Photocatalytic Degradation of Dyes: An Overview. *Current Catalysis*, **7** (2):99–121, doi 10.2174/2211544707666171219161846.

Wang, L., Ruan, Y., Diao, Z., Chen, D., and Kong, L. (2025). Catalytic degradation of Rhodamine B through peroxymonosulfate activation by the Co-doped hydroxyapatite. *Environmental Research*, **267**, doi 10.1016/j.envres.2024.120657.

Wang, Q., Sun, Y., Li, S., Zhang, P., and Yao, Q. (2020). Synthesis and modification of ZIF-8 and its application in drug delivery and tumor therapy. *RSC Advances*, **10** (62):37600–20, doi 10.1039/d0ra07950b.

Xiang, P., Tang, C., Ma, K., and Li, X. (2025). Adsorption of Rhodamine B pollutants from wastewater using MoS_2: The critical role of crystal phase regulation. *Journal of*

Water Process Engineering, **70**, doi 10.1016/j.jwpe.2025.107130.

Zheng, M., Guo, M., Ma, F., Li, W., and Shao, Y. (2025). Recent advances in graphitic carbon nitride-based composites for enhanced photocatalytic degradation of rhodamine B: mechanism, properties and environmental applications. *Nanoscale Advances*, **7** (16):4780–802, doi 10.1039/d5na00439j.